DFT Investigation of the Single-Center, Two-State Model for the Broken Rate Order of Transition Metal Catalyzed Olefin Polymerization

Vidar R. Jensen,*,† Debasis Koley,‡ Mavinahalli N. Jagadeesh,‡ and Walter Thiel*,‡

Department of Chemistry, University of Bergen, Allégaten 41, N-5007 Bergen, Norway, and Max-Planck-Institut für Kohlenforschung, Kaiser-Wilhelm-Platz 1, D-45470 Mülheim an der Ruhr, Germany

Received June 10, 2005; Revised Manuscript Received July 31, 2005

ABSTRACT: Density functional calculations have been performed on different conformers and isomers of the propyl group in alkyl cations $[L_2Zr-Pr]^+$ (L = Cp, Cp*; Pr = *n*-propyl), corresponding to two catalysts with different observed rate orders (n) for ethylene polymerization, to explore the single-center, two-state kinetic model for olefin polymerization. For L = Cp ($n \approx 1$), the β-agostic conformer is found to be the most stable structure and also the most reactive with respect to ethylene coordination, which is commensurate with unity rate order. For L = Cp* ($n \approx 1.4$), the favored propagation route involves the γ- and α-agostic conformations of the alkyl complex, with coordination taking place to an α-agostic conformation in order to minimize the steric hindrance experienced by the incoming ethylene. The barriers to rearrangement from the α- and γ-agostic conformers to the more stable β-agostic structure are significantly lower than those of propagation. Moreover, no structure was found to be of lower energy than the β-agostic conformation, and the latter thus takes the role of the resting state for both catalysts in the present study. Assuming that the single-center, two-state model applies to zirconocene-catalyzed ethylene polymerization, our calculations thus suggest that the corresponding fast and slow, or dormant, states do not originate from equilibria of the alkyl group as investigated here.

Introduction

The introduction and availability of structurally well-defined homogeneous catalysts, in particular the metallocene-based class of catalysts, has formed the basis for an impressive level of mechanistic insight into the field of transition metal catalyzed olefin polymerization. The active species in metallocene-based polymerization has been identified as a transition metal alkyl cation of the general formula $[L_2MR]^+$ (L = Cp or related ligands; M = transition metal; R = alkyl group).[1] It is clear that the determination and characterization of the active polymerizing complex have had tremendous impact on the subsequent mechanistic investigations and on the further developments in the field of olefin polymerization. The metal alkyl cation has often been the starting point for mechanistic discussions and investigations, exemplified by the numerous molecular-level computational studies that have relied on the alkylmetallocene cation as model for the active catalyst (see e.g. refs 2−11). These investigations have added detail and resolution to the propagation mechanism developed by Cossee and Arlman[12] as well as to the mechanism of most of the other key elementary reactions of olefin polymerization. The computational efforts have produced a particularly detailed picture for the reaction pathway of olefin insertion into the metal−alkyl bond from the preinsertion metal−olefin complex, highlighting the role of agostic interactions at different stages of the reaction. Results from such calculations have often compared favorably to experimental observations when such comparisons have been possible. In polymerization of propene using *ansa*-zirconocenes, for example, structural considerations limited to the central reacting cation may explain the tacticity of the polypropene formed[13] and even suffice for predictions thereof with surprisingly high accuracy.[6]

The properties of the catalyst may, however, also be heavily influenced by the degree of cation−anion association, as determined by factors such as the exact nature of the solvent or the anion.[14] The role of the cocatalyst anion has been the subject of a series of theoretical investigations and has been studied particularly intensively in recent years (see, e.g. refs 2, 4, 15−18). These modeling efforts have been facilitated and stimulated by the development of the borate family of anions and structurally well-characterized catalysts such as $Cp_2ZrPr^+(YB(C_6F_5)_3)^-$ (Y = H, CH_3).[19] The detailed control of the molecular structure of the catalyst has also been extended to synthesis of single molecule catalysts with tethered cocatalyst anions and olefins.[20,21] Such systems have allowed for the observation of insertion events using advanced NMR techniques and an unprecedented microscopic insight into the workings of the metallocene catalysts.

Despite these developments and advances, there are still mechanistic problems that remain to be solved. The perhaps most puzzling discrepancy between the existing, largely accepted, mechanism and experimental observation concerns the influence of monomer concentration on the propagation rate. The Cossee−Arlman mechanism involves the coordination and insertion of only one monomer at the time, resulting in a propagation rate law which is first-order in monomer concentration, i.e.

$$R_p = k_p[C][M]^n \quad (n = 1) \tag{1}$$

where [C] is the concentration of active centers and [M] the concentration of monomer. However, the observed reaction order with respect to monomer concentration is not restricted to unity, and rate orders higher than

† University of Bergen.
‡ Max-Planck-Institut für Kohlenforschung.
* Corresponding authors. E-mail: Vidar.Jensen@kj.uib.no; thiel@mpi-muelheim.mpg.de.

10.1021/ma051224a CCC: $30.25 © 2005 American Chemical Society
Published on Web 10/27/2005

Scheme 1

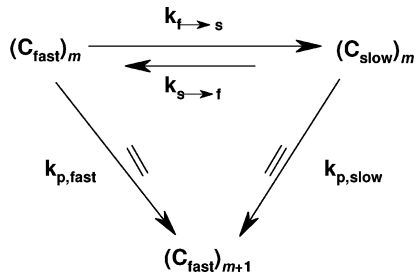

unity have been reported for a broad spectrum of catalysts and monomers.[22−24] For metallocene-based polymerizations in the homogeneous phase, all conceivable indirect effects such as mass- or heat-transfer limitations have been ruled out.[23,24] This led Mülhaupt et al.[24] to claim that the observed broken rate order must be caused by "equilibria involving the active species" and that the monomer "might be involved in an equilibrium between dormant and active catalyst sites" whereas Schaper et al.[25] pointed out that this must be due to the "intrinsic mechanisms of the polymerization catalysis". One possible mechanistic explanation for a rate order higher than unity in monomer concentration would be the simultaneous participation of more than one monomer in the propagation cycle. Mechanisms that postulate the presence of two monomers at the transition metal center have been suggested,[26] and these ideas have also been subjected to quantum chemical investigation.[2,27] However, as pointed out by Fait et al.,[28] a mechanism based on the involvement of more than one monomer is not necessary in order to obtain a rate law implying an effective order higher than one in monomer concentration. With the assumption that the active center of a catalyst exists in two states, one affording slow and the other fast propagation, it is possible to explain rate orders $1 < n < 2$.

The Single-Center, Two-State Model. The model by Fait et al.[28] places certain requirements and limitations on the allowed relative energies and kinetic constants of the propagation: (1) The catalytic center has two active, monomer-free states, C_{fast} and C_{slow}, with different propagation rate constants, $k_{p,fast}$ and $k_{p,slow}$. (2) C_{slow} has a lower free energy than C_{fast}. (3) The rate of interconversion from the fast to the slow state ($C_{fast} \rightarrow C_{slow}$) is intermediate between the rate of propagation for the fast and slow state, respectively, i.e., $k_{p,fast}[M] > k_{f\to s} > k_{p,slow}[M] > k_{s\to f}$. (4) Monomer insertion transforms C_{slow} into C_{fast}.

A propagation cycle for polymerization of ethylene adhering to these requirements is illustrated in Scheme 1, where m and $m + 1$ indicate the number of monomer units inserted into the polymer chain.

The Strategy. The single-center, two-state model is attractive in its simplicity. For example, no major revision of the Cossee−Arlman mechanism, e.g., through inclusion of a second monomer molecule, is required. The model is purely kinetic in nature, but the authors suggest that the two states of the active center "could differ in the conformation of the growing polymer chain", an explanation in agreement with the suggestions cited above,[24,25] i.e., that the reasons for the broken rate order are more likely due to mechanistic *details* such as equilibria between different species, or states, of the active catalyst. In principle, it should be possible to locate candidates for such species, for example by quantum chemical modeling. We are not aware of studies that have been specifically aimed at detecting such equilibria, but one computational study reported a stable zirconocene cation with a secondary alkyl chain to be a candidate for a slow propagating state.[5] Other computational studies have investigated possible active and dormant states arising from different adducts between $[Cp_2ZrMe]^+$, trimethylaluminum (TMA), and models of methylated methylaluminoxane, $[MeMAO]^-$.[29,30]

An attractive strategy in order to search for candidate slow and fast states could involve computational comparison of catalysts with confirmed different rate orders in monomer concentration. These catalysts should be as similar as possible and, of course, computationally tractable. An excellent pair of catalysts for this task seem to be the simple zirconocenes L_2ZrCl_2 (L = Cp, i.e., cyclopentadienyl, and L = Cp*, i.e., pentamethylcyclopentadienyl). These catalysts are structurally closely related, yet an analysis of kinetic data from two different laboratories shows that they have different rate orders, $n = 0.99$ for L = Cp and $n = 1.4$ for Cp*, for polymerization of ethylene with methylaluminoxane (MAO) as cocatalyst.[9,10] A difference of 0.4 between the two rate orders was confirmed by explicit comparison of the two catalysts in the laboratory of Gerhard Fink,[31] albeit with higher absolute values ($n = 1.3$ for L = Cp and $n = 1.7$ for Cp*), and these two catalysts were thus selected for an explicit search for slow and fast states that could possibly match the single-center, two-state kinetic model. Thorshaug et al.[9,10] have reported a detailed combined experimental and computational study of these two catalysts. A pattern of energies matching a single-center, two-state model cannot be discerned among their computational results, and a new comparative study of these two catalysts should focus on sections of the potential energy surface not covered by the investigation of Thorshaug et al.

To this end, we have performed a density functional theory investigation of different conformers and isomers of the alkyl cation models of the active centers, $[L_2Zr-Pr]^+$ (L = Cp, Cp*; Pr = *n*-propyl as the model of the growing polymer chain), of the two catalysts as well as their corresponding ethylene coordination and insertion reactions. In addition to our highly specific goal to search for potential explanations for the difference in rate order recorded for these two catalysts, the current study will focus especially on the entrance side of the potential energy surface of propagation and thereby complement earlier mechanistic studies of these metallocenes.[9,10]

Computational Details

We used gradient-corrected density functional theory (DFT) with the gradient corrections included self-consistently both during geometry optimization and energy evaluation. The local exchange-correlation potential developed by Vosko et al.[32] was augmented with Becke's[33] nonlocal exchange corrections and Perdew and Wang's[34] nonlocal correlation corrections. The resulting BPW91 functional was used in the spin-restricted formulation implemented in the Gaussian 98[35] and 03[36] set of programs. Detailed studies show that the BPW91 functional is capable of providing accurate energy profiles for the monomer insertion step during metal-catalyzed olefin polymerization.[37] Some validation calculations (where indicated) were performed, using the

Gaussian set of programs with the three-parameter hybrid density functional method of Becke (termed "B3LYP")[38] and with the coupled-cluster approximation including single and double excitations and with contributions from connected triples added perturbatively (CCSD(T)).[39] All valence electrons were correlated in the CCSD(T) calculations.

In the geometry optimizations, effective core potentials (ECP)[40] for the small Ar core of zirconium and the small Ne core of titanium were used in combination with valence basis sets contracted to [3s,3p,2d].[40] For aluminum, an ECP[41] was used for the Ne core in combination with a [2s,2p] contracted valence basis[41] set extended with a polarization function ($\alpha_d = 0.325$). Oxygen, carbon, and hydrogen atoms were described by standard Dunning−Hay[42] valence double-ζ basis sets, with a scale factor of 1.2 (1.15) applied for the inner (outer) exponents of H. Polarization functions were added to O ($\alpha_d = 0.961$) atoms and to C ($\alpha_d = 0.75$) atoms of the ethylene or the polymer chain. The Gaussian 98 defaults[35] were applied for convergence criteria whereas the "ultrafine" (99,590) grid was used in numerical integrations. Each stationary point was characterized by analytic calculation of the second-derivative matrix. Zero-point and thermal corrections to the energies were computed from the harmonic frequencies using standard procedures. The $T\Delta S$ contributions calculated for ethylene coordination in the gas phase (10−12 kcal/mol) at 298.15 K do not reflect the actual entropic cost of binding the olefin to the catalyst complex in solution. The discrepancy can be reduced by taking into account the solvation entropy of ethylene since the solvation entropies of the catalyst complex with and without ethylene should be similar.[43] The ethylene solvation entropy amounts to 15.4 eu in toluene,[44] equivalent to 4.6 kcal/mol at 298.15 K, or ca. 40% of the calculated gas-phase value for $T\Delta S$. Similar reasoning leads to the same percentage (40%) for the solvation entropy of H_2 in toluene. The entropic cost of olefin and dihydrogen coordination to or elimination from the transition metal complex in solution (toluene) has thus been approximated by 60% of the corresponding gas-phase values. This correction strategy has been applied also to transition states of coordination/elimination and is expected to be a good estimate of the true entropy contribution in condensed phase.[43]

All energies reported in the current work are based on single-point energy calculations using basis sets that were improved compared to those of the geometry optimizations described above: C and H atoms of the ethylene or the polymer chain were described by augmented Dunning triple-ζ sets denoted TZD2P[37] to account for known basis set sensitivities,[37] and polarization functions were included for the C atoms of the Cp rings ($\alpha_d = 0.75$). The outermost primitive was split off from each of the contracted 5s, 5p, and 5d functions in the Zr valence basis set described above to give a final [4s,4p,3d] basis set involving 311, 111, and 211 contractions for the 5s, 5p, and 5d functions, respectively. Titanium was described by Wachters (14s,11p,6d) primitive basis set extended by (6f)[45] and contracted to [8s,7p,4d,2f], whereas hydrogen atoms directly bound to Ti were described by Dunning basis sets contracted to [3s,1p] as described in ref 37. The SCF convergence criterion used for these single-point calculations was 10^{-5} (rms density change), and the "ultrafine" (99,590) grid was used for the numerical integrations. With the above-described method and basis sets for energy evaluation, the basis set superposition errors (BSSEs) of the Zr−ethylene interaction in zirconocene π complexes, $[Cp_2Zr-Pr(C_2H_4)]^+$, were calculated to be 1.1 and 1.2 kcal/mol for the β- and α-agostic conformations, respectively, using the counterpoise method. Our computational protocol thus gives small BSSEs that do not affect the calculated relative stabilities to any significant

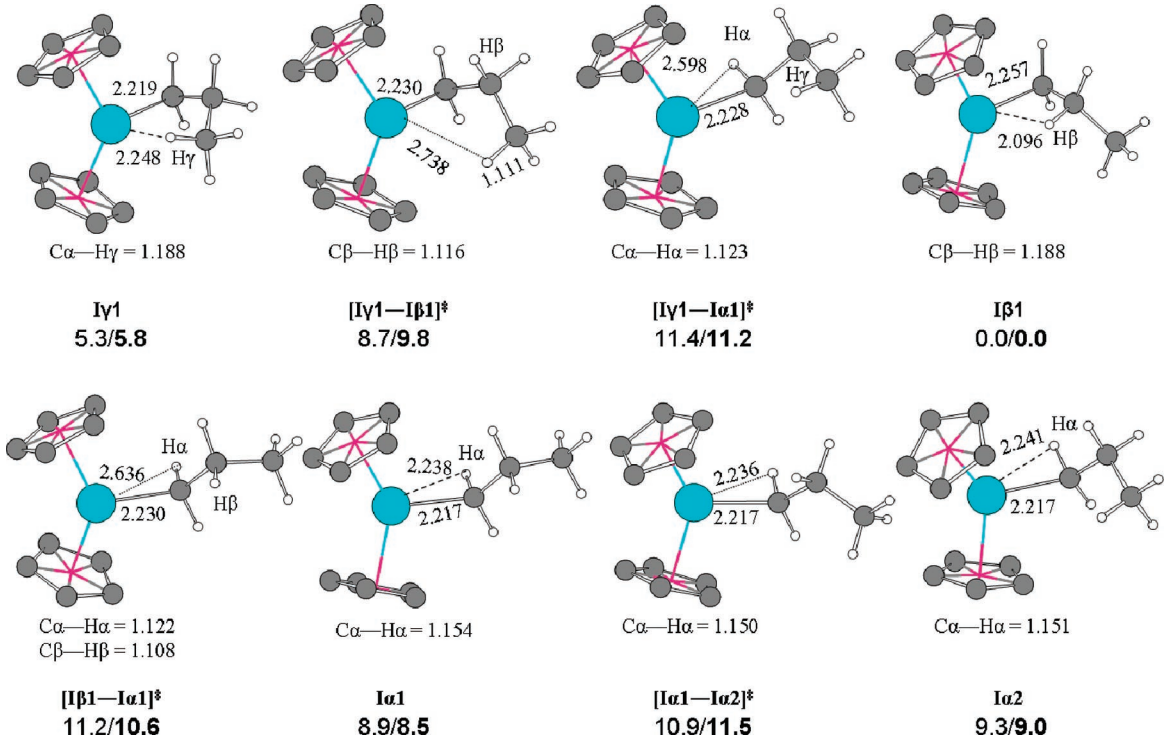

Figure 1. Different conformers of the primary alkyl cation, $[Cp_2Zr-Pr]^+$, and the corresponding transition states of their interconversion. Bond distances are given in angstroms, whereas energies are given in kcal/mol ($\Delta H_{298}/\Delta G_{298}$) relative to **I$\beta$1** and free ethylene. Hydrogen atoms of the Cp ligands have been omitted for clarity.

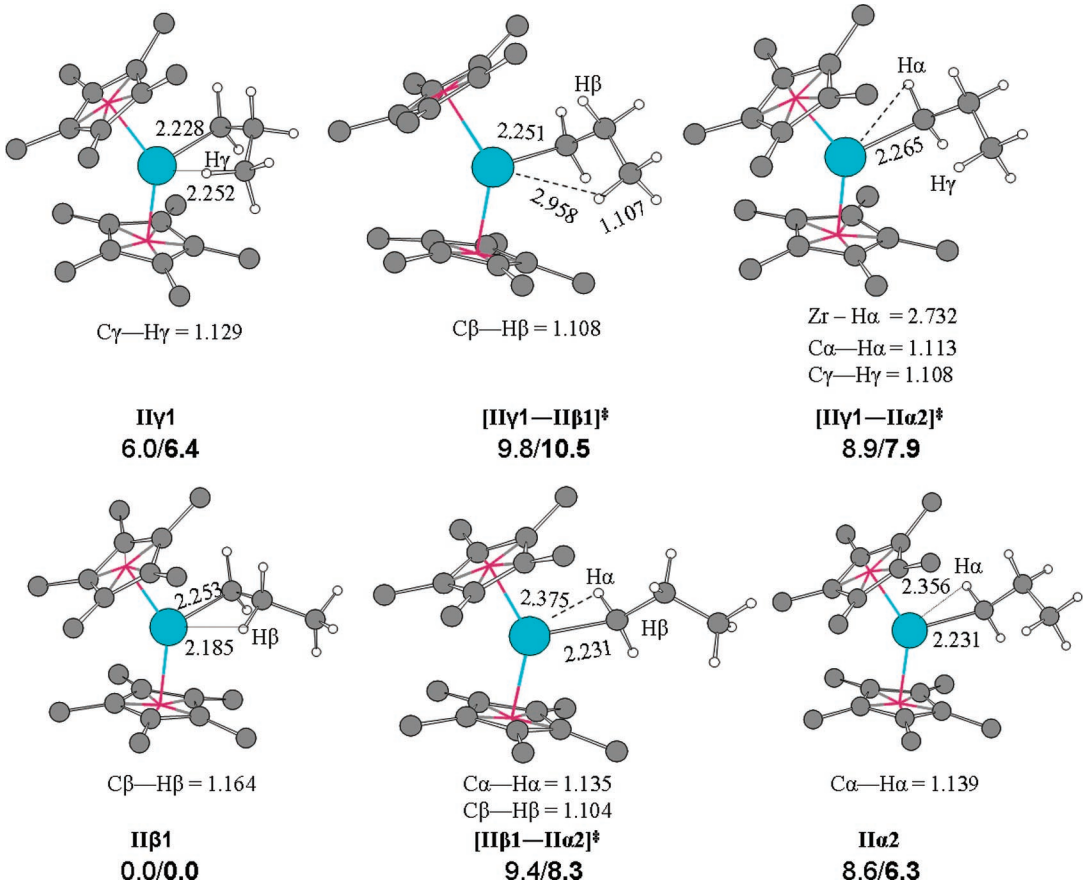

Figure 2. Different conformers of the primary alkyl cation, $[Cp^*_2Zr{-}Pr]^+$, and the corresponding transition states of their interconversion. Bond distances are given in angstroms. Energies are given in kcal/mol (ΔH_{298}/ΔG_{298}) relative to **II*β*1** and free ethylene. Hydrogen atoms of the Cp* ligands have been omitted for clarity.

extent, and estimates thereof are therefore not included in the current contribution.

Results and Discussion

In the following we will present computational results for the various elementary reactions of the monomer-free alkyl cations, $[L_2Zr{-}Pr]^+$ (L = Cp, Cp*; Pr = *n*-propyl), as well as its coordination and insertion of ethylene. We will compare our results with published computational and experimental data and with the pattern required for the single-center, two-state model (vide supra), at first assuming that the slow center can be identified among the conformations formed by the *n*-propyl with the zirconocene fragment L_2Zr. Finally, we will also investigate the possibility of generating a slow state by isomerization of the *n*-propyl group. Structures involving L = Cp are labeled by a leading "**I**" and those of L = Cp* by "**II**". In the case of an agostic Zr−H−C structure, this is followed by a Greek letter identifying the carbon atom involved.

Primary Alkyl Cations. The calculated structures and relative energies of zirconium alkyl cations $[Cp_2Zr{-}Pr]^+$ with primary alkyl groups in α-, *β*-, and *γ*-agostic conformations, and their respective unimolecular interconversion reactions are shown in Figure 1, whereas the corresponding results for $[Cp^*_2Zr{-}Pr]^+$ are given in Figure 2. The usual order with respect to relative stability of these three conformations for zirconocenes emerges from our calculations, with the *β*-agostic structure being the most and the α-agostic the least stable structure. The free energy difference between these two structures amounts to more than 8 kcal/mol for L = Cp and more than 6 kcal/mol for L = Cp*. The stability for the *β*-agostic structure is reflected in the structures, with the C*β*−H*β* bond being elongated by 6−9 pm due to the agostic interaction (see Figures 1 and 2). For the Cp* complex, however, the *γ*- and α-agostic conformations are in fact of similar energies. The stabilization of the α-agostic structure with respect to the other two conformations upon going from L = Cp to Cp* is due to destabilization of pyramidal (bent) structures for the three-coordinate metal complex, $[L_2Zr{-}Pr]^+$ for bulkier ligands, L. The α-agostic structure **IIα2** is planar, Θ = 0.0°,[46] whereas the other agostic structures are more pyramidal, with deviations from planarity of Θ = 3.0° (**II*β*1**) and Θ = 9.8° (**II*γ*1**).

It should also be noted that the most stable (by 0.5 kcal/mol) α-agostic conformation located for L = Cp (structure **Iα1**, Figure 1) is, in fact, not a minimum for L = Cp*. The conformation of the propyl chain in **Iα2** (**IIα2**) is similar to that of **I*γ*1** (**II*γ*1**) (see below for the interconversion between **Iα2** and **I*γ*1**), whereas **Iα1** can be generated from **Iα2** by a facile ∼180° rotation ($\Delta G^{\ddagger}_{298}$ = 2.5 kcal/mol relative to **Iα2**) of the terminal ethyl group around the Cα−C*β* bond. This rotation places a *β*-agostic hydrogen in position for coordination to the metal through the base of the L_2ZrPr pyramid. Because the L_2ZrPr fragment is planar in the case of L = Cp* (Θ = 0.0° for **IIα2**), access to the metal atom from the base of the pyramid is easier than for L = Cp (Θ = 11.5° for **Iα2**). Relaxation to **II*β*1** is thus the reason for the lack of stability for this α-agostic conformation of the chain for the bulkier Cp* ligand.

We have located transition states for interconversion between pairs of agostic structures for both L = Cp and Cp*. Interconversion between the primary product of ethylene insertion, **Iγ1**, and the most stable conformation, **Iβ1**, is dominated by rotation around Cα−Cβ and proceeds with a free energy barrier of ca. 4 kcal/mol for L = Cp or close to 10 kcal/mol for the reverse reaction. Slightly more energy (ca. 5 kcal/mol) is needed to overcome the barrier to give the α-agostic reactant, **Iα1**, directly from the γ-agostic reactant through widening of the Zr−Cα−Cβ angle by more than 50°. In contrast, more than 10 kcal/mol is required to overcome the corresponding barrier from **Iβ1**. For L = Cp*, the stabilization of the α-agostic conformation for the sterically more demanding ligand results in a lowering of barriers to forming the α-agostic conformation from both of the other two conformations, to below 2 kcal/mol in order to reach **[IIγ1−IIα2]**‡. The corresponding barrier starting from **IIβ1** is higher than 8 kcal/mol. Our results for the γ- and β-agostic structures and their interconversion are comparable to those of Thorshaug et al.,[9] whereas the stabilization of the α-agostic structure for the $[Cp^*_2Zr-Pr]^+$ complex and the lowering of the barriers for its formation have apparently not been reported previously.

We now turn to the question of whether the pattern seen for these unimolecular rearrangements could be commensurate with the interconversions described by Fait et al.[28] for a single-center, two-state mechanism. For both catalysts, the only candidate so far for C_{slow} is the β-agostic structure. The primary, kinetic product of insertion, the γ-agostic conformation, **Iγ1**, seems to be an interesting candidate for C_{fast}, provided that the subsequent coordination and insertion of ethylene proceed with lower barriers than the unimolecular conversion to the β-agostic conformation. In addition, for L = Cp, coordination of ethylene would have to take place for **Iγ1**, and not for **Iα1**, because the barrier to formation of **Iβ1** (the assumed C_{slow}) is lower than that for formation of **Iα1**. Thorshaug et al. reported virtually barrierless coordination of ethylene to γ-agostic alkyl cations $[Cp_2Zr-R]^+$, making this scenario seem possible. For L = Cp*, the α-agostic species may in principle be responsible for the "fast" reaction with ethylene since its formation from **IIγ1** (C_{fast}) is associated with the lowest of all the interconversion barriers calculated for the present primary propyl cations. Thus, our results for the ethylene-free alkyl cations indicate that ethylene approach to the catalyst complex should be explicitly investigated for all three agostic conformations and that the α-agostic conformer in particular may turn out to be important for $[Cp^*_2Zr-Pr]^+$.

Frontside Olefin Coordination and Insertion.[47] We start this section by considering coordination of ethylene to the candidate fast state discovered above, the γ-agostic conformation for L = Cp, **Iγ1**. However, our calculations suggest that approach of ethylene to this conformer is less favored than other modes of monomer approach and is associated with a free energy barrier of 7.2 kcal/mol relative to **Iγ1** (12.9 kcal/mol relative to **Iβ1**, cf. Figure 3). The major part of this barrier arises from the entropic costs (5.5 kcal/mol) of approaching an ethylene molecule toward the apex of the L_2ZrPr pyramid which is essentially covered by the propyl chain (see Figure 3). The electronic contribution (1.7 kcal/mol) is very similar to the energy barriers of Thorshaug et al.[9] for $[Cp_2Zr-Pr]^+$. Taking into account their reported increase in the electronic barrier to coordination for Zr cations with longer (and more realistic) alkyl chains than propyl, we can safely assume that the true free energy barrier for ethylene coordination to realistic γ-agostic complexes is higher than that reported here and that coordination to this conformer is unimportant.

In contrast, ethylene coordination to the two other conformations of the growing polymer chain results in transition structures that are significantly less sterically crowded and thus more stable.[48] Coordination to the β-agostic reactant is even thermoneutral and barrierless relative to **Iβ1**.[49] For L = Cp, our gas-phase calculations predict that the γ-agostic kinetic product of ethylene insertion rearranges ($\Delta G^{\ddagger}_{298}$ = 4.0 kcal/mol) to the more stable β-agostic conformer and that ethylene coordinates to the latter species without a barrier.

The unfavorable coordination to **Iγ1** for L = Cp induced us not to investigate coordination of ethylene to **IIγ1** since the crowding of the pentamethyl-substituted analogue is expected to be even more pronounced. The results for coordination to the β- and α-agostic species support this expectation (see Figure 4). Coordination to the sterically more demanding Cp* analogue preferably takes place when the propyl group has the least possible association with the metal atom, namely the α-agostic structure, **IIα2**. The free energy barrier for this complexation is 7.2 (13.5) kcal/mol relative to **IIα2** (**IIβ1**), lower than the corresponding barrier (14.2 kcal/mol) of coordination to **IIβ1**. Thus, for L = Cp*, our gas-phase calculations predict that the γ-agostic kinetic product of ethylene insertion rearranges ($\Delta G^{\ddagger}_{298}$ = 1.5 kcal/mol) to the α-agostic conformer and that ethylene coordinates to the latter species (via TS **[IIα2−IIFα1]**‡) with a low barrier,[50] in contrast to the clear preference for coordination to the β-agostic reactant seen for L = Cp. A growing polymer chain in an α-agostic conformation shields the metal against attack from an olefin to a lesser extent than a chain in a β- or γ-agostic conformation (Figures 3 and 4). The preferred type of ethylene coordination (β for L = Cp vs α for L = Cp*) thus depends on the steric hindrance experienced by the approaching olefin. A similar preference for olefin coordination to the α-agostic alkyl cation has been noted already for half-sandwich Cr(III)-based catalysts for ethylene oligomerization[51] but has, to our knowledge, not previously been reported for zirconocenes.

For L = Cp, the β- and α-agostic π-complexes are of similar stability, and the interconversion between them is facile, with a free energy barrier of 2.7 kcal/mol from **IFβ1**. There exist several frontside α-agostic π-complexes that are slightly less stable than **IFα1**. They differ mainly in their relative ethylene−propyl conformations (structures not reported), and their interconversions are facile. The lowest energy path of ethylene insertion starts from a frontside α-agostic π-complex[52] and is triggered by a rotation ($\Delta G^{\ddagger}_{298}$ = 2.3 kcal/mol relative to **IFα1**) around the Zr−Pr bond to obtain an α-agostic interaction opposite to ethylene. No minimum exists for this conformation, and insertion of ethylene proceeds without barrier after passing the TS of rotation around the Zr−Pr bond, **[IFα1−IγP]**‡. A Cα−Hα bond distance of 1.119 Å indicates the beginning formation of a backside Zr−Hα agostic interaction that assists insertion and later manifests itself as a γ-agostic bond in the Zr−pentyl insertion product (**IγP**, Figure 3).

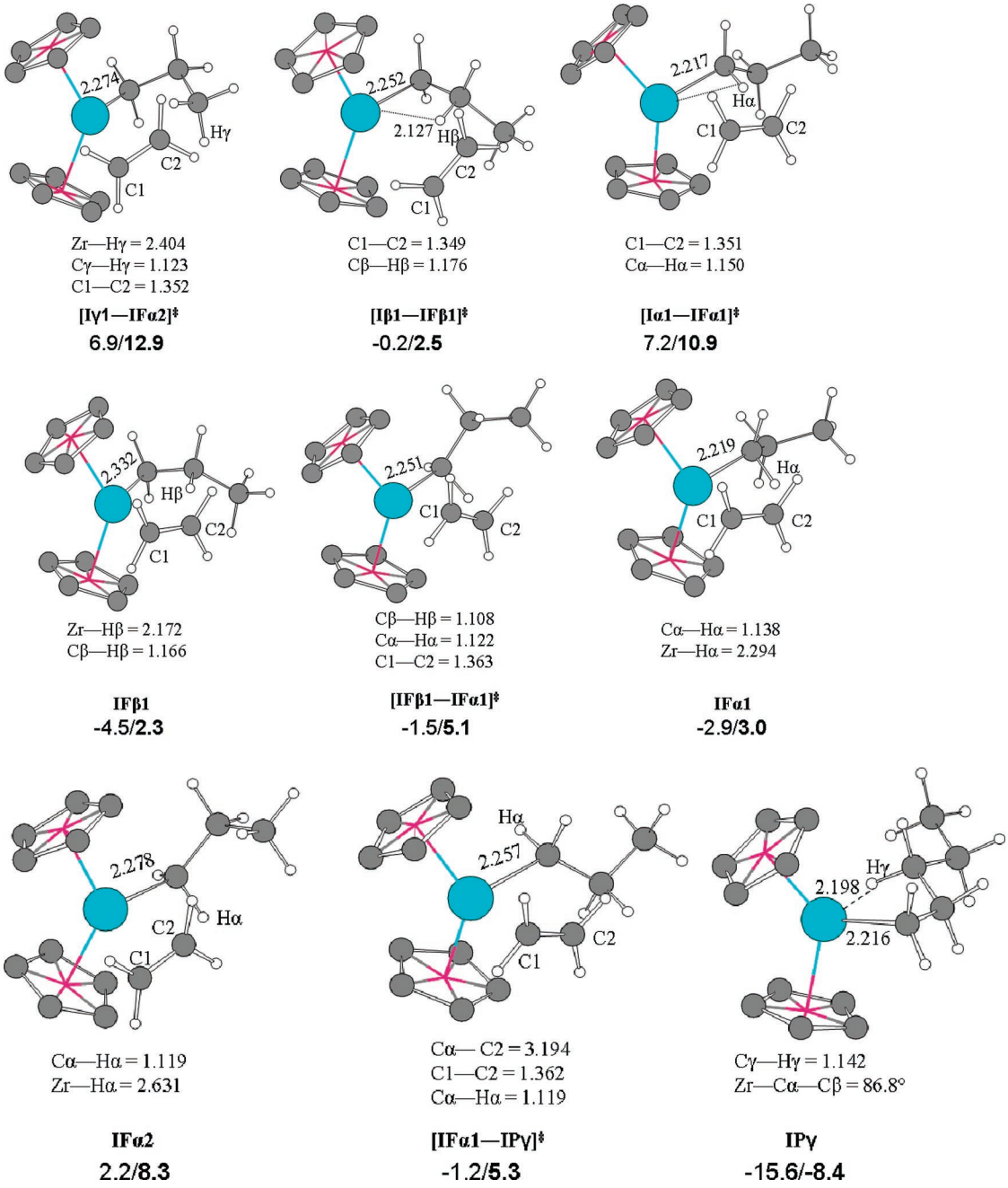

Figure 3. Transition states and minima along the pathway of frontside ethylene coordination and insertion for $[Cp_2Zr-Pr]^+$. Bond distances are given in angstroms, whereas energies are given in kcal/mol ($\Delta H_{298}/\Delta G_{298}$) relative to the **I*β*1** and free ethylene. Hydrogen atoms of the Cp ligand have been omitted for clarity.

For L = Cp*, the most stable π-complex is in fact α-agostic (see structure **IIFα1**, Figure 4). A second α-agostic π-complex, **IIFα2** (Figure 4), has the propyl group in the same conformation as in **IIα2** and is 5.3 kcal/mol less stable than **IIFα1**. The high energy of **IIFα2** indicates that this π-complex is unimportant for propagation, and therefore ethylene coordination and insertion have not been investigated for this conformation of the propyl group. Ethylene insertion for **IIFα1** is facile, with a barrier from the π-complex of 4.9 kcal/mol, or 17.6 kcal/mol relative to **II*β*1**.

Backside Olefin Coordination and Insertion.[47] For sterically less crowded constrained-geometry catalysts, barriers to frontside and backside insertion have been found to be similar,[11] whereas for metallocenes, the backside approach seems to be unimportant. Lohrenz et al.[52] noted already 10 years ago that "backside insertion, although feasible, has a higher activation barrier than the frontside propagation, and is entropically disfavored." Similar results were reached both for L = Cp and Cp* in the comparative study of ethylene polymerization with $[L_2Zr-R]^+$ conducted by Thorshaug et al.,[9] who noted that "backside insertion to a β-agostic conformation is very unlikely for L = Cp*." These results suggest that it is not worthwhile to investigate the backside approach to β- or γ-agostic conformations of the alkyl cation over again for the present zirconocenes. On the other hand, since ethylene coordination to the α-agostic conformation is most favorable for the bulky system, L = Cp*, one may expect the backside approach to be feasible in this case. We indeed find that such backside approach of ethylene to the pentamethyl-substituted zirconocene results in direct insertion (i.e., not passing through a π-complex) with a barrier relative

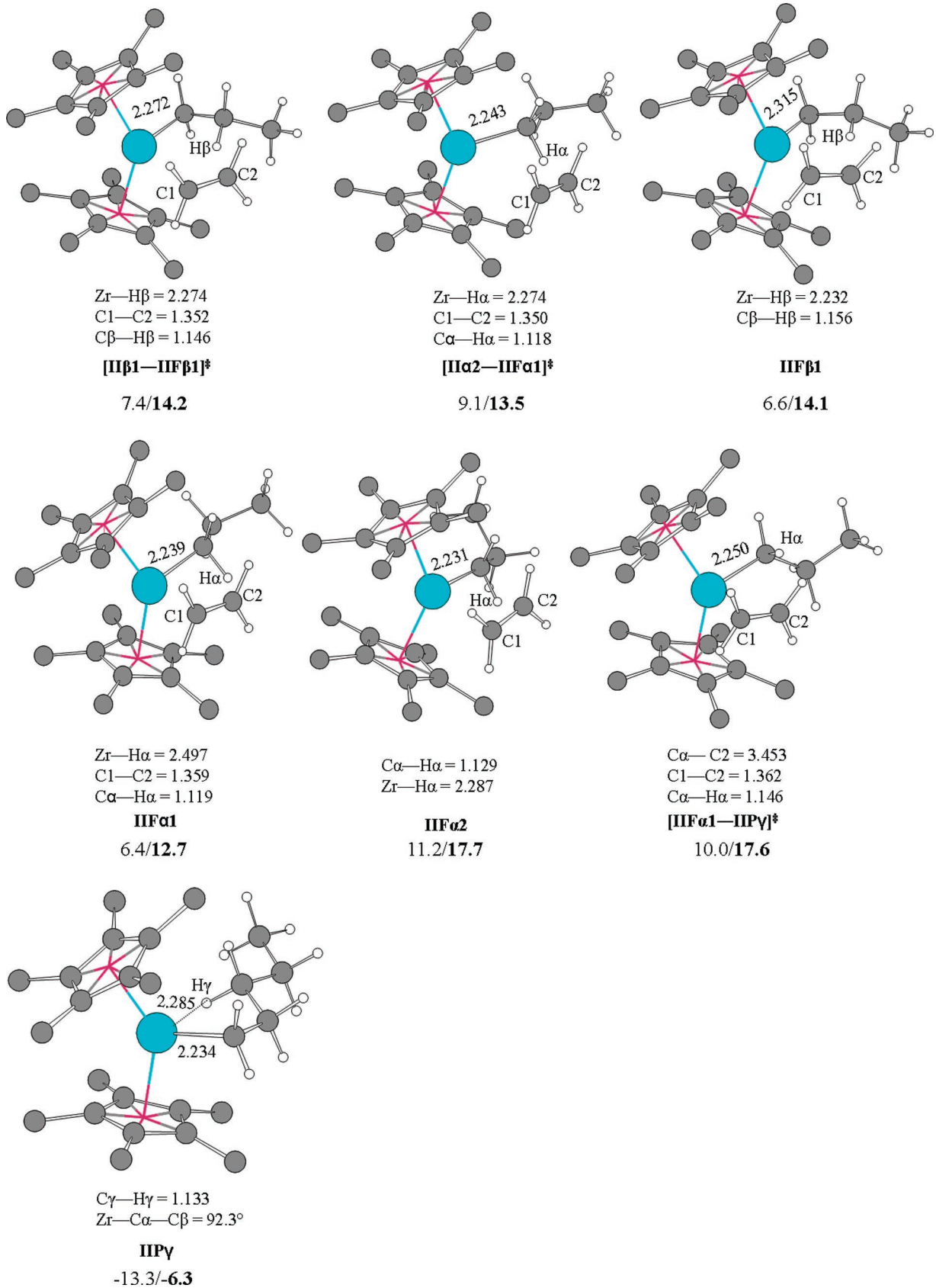

Figure 4. Transition states and minima along the pathway of frontside ethylene coordination and insertion for $[Cp^*_2Zr-Pr]^+$. Bond distances are given in angstroms, whereas energies are given in kcal/mol ($\Delta H_{298}/\Delta G_{298}$) relative to **II*β*1** and free ethylene. Hydrogen atoms of the Cp* ligands have been omitted for clarity.

to **II*β*1** which is less than 1 kcal/mol higher than that estimated for frontside insertion. The TS occurs much earlier than typical four-center transition states of olefin insertion (see structure **[IIα2−IIP*γ*]**‡ in Figure 5). The C−C bond of the inserting ethylene (1.349 Å) is not elongated compared to the bond in free ethylene, and

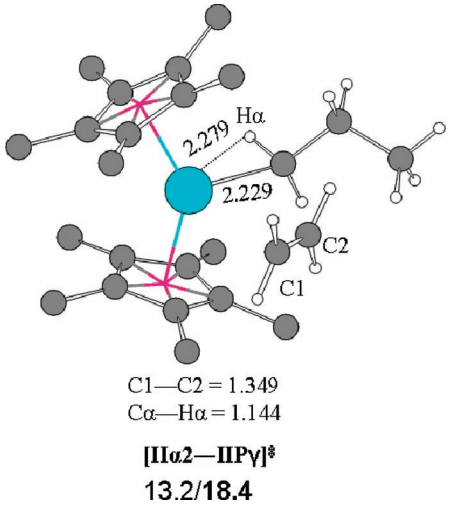

Figure 5. Transition state for direct backside ethylene insertion for $[Cp^*_2Zr-Pr]^+$. Bond distances are given in angstroms, whereas energies are given in kcal/mol (ΔH_{298}/ΔG_{298}) relative to the corresponding β-agostic primary alkyl cation (**IIβ1**) and free ethylene. Hydrogen atoms of the Cp* ligands have been omitted for clarity.

the bond to be formed during insertion (C2−Cα) is very long (3.886 Å). Thus, we have located feasible frontside and backside routes of olefin coordination and insertion for the active species $[Cp^*_2Zr-Pr]^+$, which in both cases has an α-agostic conformation of the propyl group.

For the Cp analogue, the feasibility of backside ethylene approach to an α-agostic conformation seems more questionable (see Figure 6). Ethylene coordination to **Iα2** is associated with a substantial free energy barrier (14.2 kcal/mol relative to **Iβ1**), whereas frontside coordination to **Iβ1** was found to be practically barrierless. Coordination leads to the formation of a π-complex, **IBα2** ($\Delta G^{\ddagger}_{298}$ = 7.2 kcal/mol relative to **Iβ1**), with the C−C bond of ethylene being far from parallel to the Zr−propyl bond and not to direct insertion. However, only a tiny barrier from this π-complex ($\Delta G^{\ddagger}_{298}$ = 0.3 kcal/mol) must be overcome in order for insertion to take place. The high barrier for ethylene coordination, however, excludes this route as part of the propagation mechanism.

Comparison to the Single-Center, Two-State Model. So far, we have assumed that both the slow and fast states of the catalyst, if they exist, are to be found among the conformations formed by the *n*-propyl group with the zirconocene fragment, L_2Zr. For L = Cp, our calculations show that the most stable of the ethylene-free complexes is also the most reactive state with respect to ethylene coordination, a pattern which is clearly not commensurate with that required for the single-center, two-state model (Scheme 1).

For L = Cp*, the situation looks better at first glance. We have already pointed out that a propagation involving fast rearrangement from the kinetic product of ethylene insertion, **IIγ1**, to the α-agostic species may be a viable route since the corresponding formation of the more stable **IIβ1** conformer involves a higher barrier. Now it turns out that ethylene coordination preferably takes place to the α-agostic reactant for L = Cp*, which further seems to strengthen the idea that the γ-agostic conformation of the alkyl cation may be a candidate for the fast state. The transformation $C_{fast} \rightarrow C_{slow}$ would then correspond to rearrangement from the γ- to the β-agostic, and from the α- to the β-agostic conformation, with barriers amounting to 4.1 and 2.0 kcal/mol, respectively. These reactions should be slower than that of fast propagation according to point 3 among the requirements of the kinetic model (vide supra). However, as explained above, the calculated propagation barriers for ethylene polymerization with $[Cp^*_2Zr-Pr]^+$ are estimated to be in the range 17−18 kcal/mol (frontside approach) and 18−19 kcal/mol (backside approach) relative to the most stable, β-agostic, conformation of the propyl cation, or 9−10 kcal/mol and 12−13 kcal/mol, respectively, relative to the α-agostic conformation. The differences between the barriers for $C_{fast} \rightarrow C_{slow}$ and propagation thus appear far too large for the corresponding rates to become comparable as a result of high monomer concentration.

One should keep in mind, of course, that the computed free energy change resulting from ethylene binding to the metal complex is associated with inaccuracies. The largest of these inaccuracies is the entropic cost of ethylene capture as obtained in our gas-phase calculations, which has been corrected (reduced) by the ethylene solvation entropy as described under Computational Details. It is difficult to see how a further (reasonable) reduction of the entropic cost or other corrections could reduce the propagation barriers of ethylene coordination and insertion enough to be comparable with the barriers to formation of the β-agostic conformation from the γ- and α-agostic conformations, i.e., with the barriers for $C_{fast} \rightarrow C_{slow}$.

Comparison to Experiment. Our gas-phase calculations thus suggest that the β-agostic alkyl cation can be regarded as a resting state for both catalysts, but that the preferred pathways of ethylene approach are different in the two cases. For L = Cp, ethylene coordinates to the β-agostic resting state, whereas ethylene complexation for L = Cp* preferably involves an α-agostic conformation. Thorshaug et al.[9] reported observed activation energies corrected by kinetic modeling in order to separate effects from propagation and deactivation, but the resulting barriers to propagation of 14.6 kcal/mol for L = Cp and 4.1 kcal/mol for L = Cp* were found to differ from their computed DFT barriers of 2−5 and 6−8 kcal/mol, respectively.[9] According to our present DFT calculations, insertion does not require enthalpic activation for L = Cp, whereas there is an enthalpic insertion barrier of ca. 9−10 kcal/mol for the bulkier catalyst with L = Cp*. Compared with the corrected experimental activation energies,[9] the available two sets of computed DFT barriers are thus too low by 10−15 kcal/mol for L = Cp and too high by 2−6 kcal/mol for L = Cp*. Uncertainties with respect to the accuracy of the presently applied density functional method as well as of the measured barriers to propagation suggest that a close agreement between the theoretical and experimental barrier heights should not be expected. However, at least for L = Cp, the difference seems large enough to warrant explanation. We note that the Cp* ligands should afford a better separation of the catalyst−cocatalyst ion pairs in solution than the smaller Cp rings, and therefore gas-phase model calculations are expected to be more realistic (smaller errors) for L = Cp*. It is reasonable to believe[9] that the poor agreement for L = Cp in the gas-phase calculations results from the lack of counterion and solvent. Nifant'ev et al.[16] have reported a thorough comparison of the energy coordination and insertion profiles for the naked zirconocene ethyl cation with those including two dif-

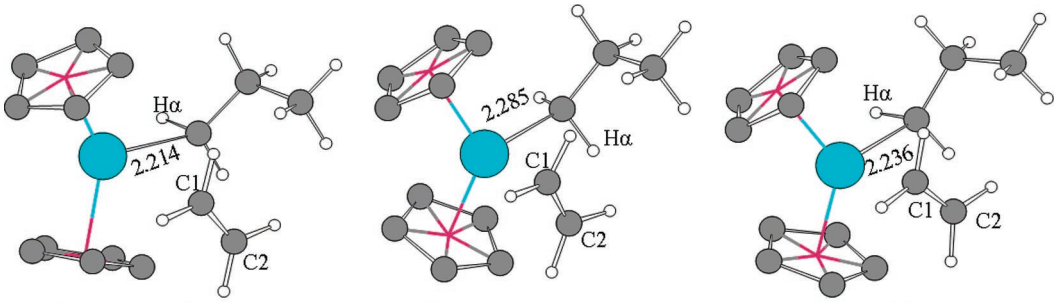

Cα—Hα = 1.158
Zr—Hα = 2.208
C1—C2 = 1.349
Cα—Zr—C2—C1 = 122.7
X1—Zr—X2 = 137.8
Θ = 2.3

[Iα2—IBα2]‡
10.3/14.2

Cα—Hα = 1.113
Zr—Hα = 2.729
C1—C2 = 1.365
Zr—Cα—Cβ = 125.3
Cα—Zr—C2—C1 = 112.9
X1—Zr—X2 = 129.3
Θ = 23.6

IBα2
0.7/7.2

Cα—Hα = 1.135
Zr—Hα = 2.408
C1—C2 = 1.364
Cα—Zr—C2—C1 = 123.1
X1—Zr—X2 = 132.2
Θ = 14.3

[IBα2—IPγ]‡
0.6/7.5

Figure 6. Transition states and minima along the pathway of backside ethylene coordination and insertion for $[Cp_2Zr{-}Pr]^+$. Bond distances are given in angstroms, whereas energies are given in kcal/mol ($\Delta H_{298}/\Delta G_{298}$) relative to the corresponding β-agostic primary alkyl cation (**Iβ1**) and free ethylene. Hydrogen atoms of the Cp ligands have been omitted for clarity.

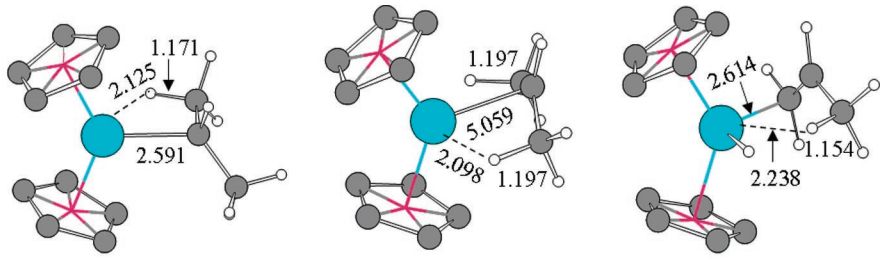

ISβ1
3.1/2.9

ISβ2
1.5/3.0

IH1
8.3/9.3

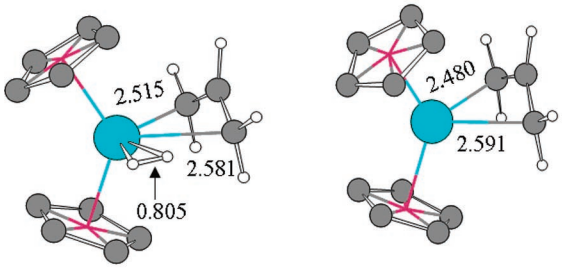

IH2
6.9/8.4

IA
11.3/7.0

Figure 7. Minima resulting from isomerization of $[Cp_2Zr{-}Pr]^+$. Bond distances are given in angstroms, whereas energies are given in kcal/mol ($\Delta H_{298}/\Delta G_{298}$) relative to the corresponding β-agostic primary alkyl cation (**Iβ1**) and free ethylene. Hydrogen atoms of the Cp ligands have been omitted for clarity.

ferent borate anions for the system $Cp_2ZrEt^+A^-$ (A^- = counterion). For the least nucleophilic borate, A^- = $B(C_6F_5)_4^-$, which is expected to show similarities to methylaluminoxane (MAO), their enthalpic propagation barrier, corresponding to ethylene coordination to $Cp_2ZrEt^+A^-$, is also close to zero and thus far from the experimental activation energy for Cp_2ZrCl_2/MAO. It appears that a more realistic modeling of metallocene-catalyzed polymerization, through inclusion of counterion, solvent, and dynamic effects,[4,15−17] will be required to clarify these discrepancies.

Isomerization of the Primary Alkyl Cations. As discussed above, our calculations suggest that equilibria between the different conformers of the *n*-propyl chain do not correspond to the fast and slow states appearing in the kinetic model of Fait et al.,[28] mainly because the rearrangements from the γ- and α-agostic conformations to the more stable β-agostic conformations are associated with low barriers. The existence of an active state more stable than the β-agostic conformer, i.e., an alternative C_{slow}, however, may lead to a pattern consistent with the single-center, two-state model. There are of course many possible structures that may turn out to have lower energies than the β-agostic state, and the present study will be limited to isomerization reactions of the Zr−alkyl cation that have already been reported to lead to structures with stabilities comparable to the β-agostic conformation.

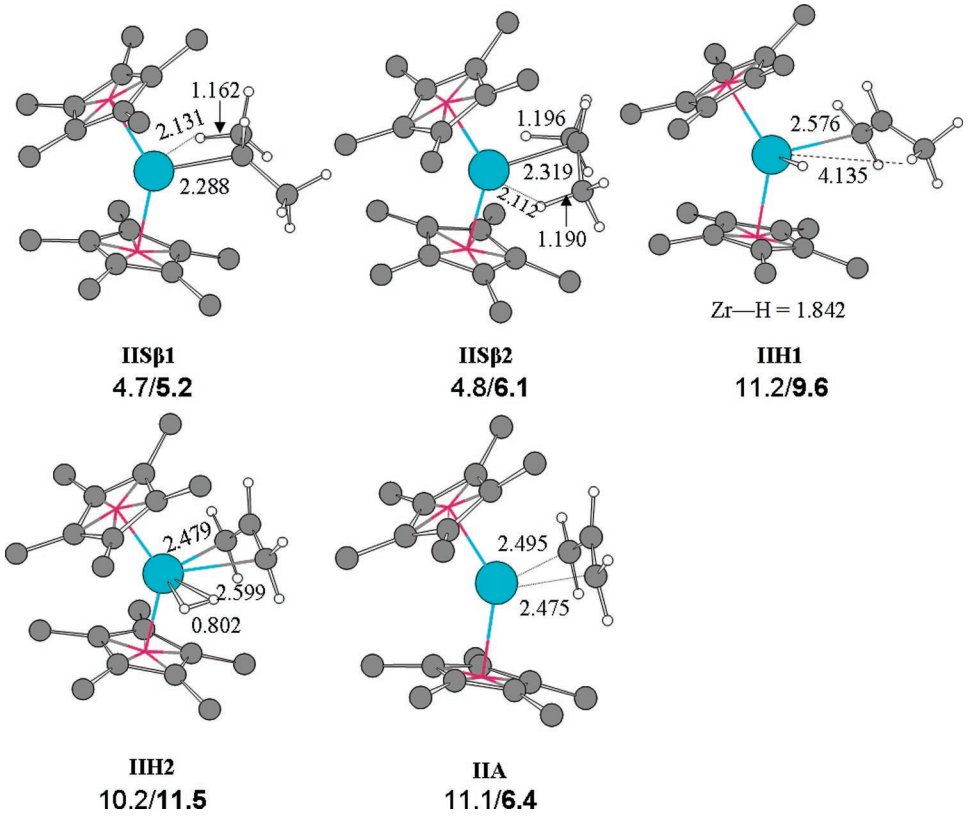

Figure 8. Minima resulting from isomerization of $[Cp^*_2Zr-Pr]^+$. Bond distances are given in angstroms, whereas energies are given in kcal/mol (ΔH_{298}/ΔG_{298}) relative to the corresponding β-agostic primary alkyl cation (**II*β*1**) and free ethylene. Hydrogen atoms of the Cp* ligands have been omitted for clarity.

One possible isomerization is initiated by β-hydrogen transfer from the alkyl chain to the metal. Subsequent rotation of the thus formed olefin and reinsertion into the metal−hydrogen bond affords a secondary metal−alkyl species. On the basis of hybrid DFT/MM calculations on propene polymerization with the catalyst *rac*-$Me_2C(3\text{-}^t\text{Bu-Ind})_2ZrCl_2$/MAO, Moscardi et al. claimed[5] that the zirconocene complex with a secondary alkyl group represents a suitable model for the catalyst resting state, i.e., for the slow state. Given that a broken rate order has been observed for a large variety of polymerization catalysts (and monomers), it is reasonable to believe that these catalysts should have similar fast and slow states. We thus decided to investigate the stability of complexes with an isopropyl group, i.e., $[L_2Zr-CH(CH_3)_2]^+$ (L = Cp, Cp*), relative to **I*β*1** and **II*β*1**. Moscardi et al. found that their secondary alkyl species, with two β-agostic hydrogen atoms, was 1 kcal/mol more stable than the corresponding primary β-agostic alkyl. In contrast, we observe a preference for the primary alkyl complex over secondary alkyl complexes with one and two β-agostic hydrogen atoms, by 3 kcal/mol for L = Cp (cf. Figure 7) and 5−6 kcal/mol for L = Cp* (Figure 8). Our results for the relative stability of primary and secondary zirconium−alkyl species thus agree with those reported by several other authors (see e.g. refs 7, 9, 53), and it seems doubtful whether secondary or tertiary alkyl species of early transition metals can be more stable than primary ones except in very special cases.[53]

Margl et al.[8] observed the formation of a stable titanium−dihydrogen complex while performing an ab initio molecular dynamics study of β-hydrogen elimination from the alkyl chain to titanium in a constrained-geometry catalyst. Subsequent elimination of H_2 leads to a cationic metal−allyl complex that is also suggested to have considerable stability.[8,17,20,54] For L = Cp, the present calculations suggest that the zirconium−olefin hydride complex (**IH1**, the product of the first hydrogen elimination to the metal) and the metal−allyl dihydrogen complex (**IH2**) are of similar free energy, ~9 kcal/mol less stable than **I*β*1**, whereas the metal−allyl complex (**IA**) is ca. 7 kcal/mol less stable than **I*β*1**. The increased steric bulk of the Cp* ligands results in destabilization of the hydride and dihydrogen structures **IIH1** and **IIH2** with respect to both the β-agostic structure **II*β*1** and the allyl complex **IIA**. The latter structure still remains ca. 6 kcal/mol less stable than the β-agostic resting state in terms of free energy where the entropy change associated with elimination of H_2 has been corrected (reduced) by 40% as described under Computational Details. If one adopts the uncorrected gas-phase entropy change, the allyl complex is only 2 kcal/mol less stable than the β-agostic resting state, **II*β*1**. The slight preference for the β-agostic complex over the allyl structure is confirmed with a hybrid method (B3LYP), which predicts a 1 kcal/mol larger energy difference. The applicability of density functional methods at describing relative stabilities between agostic metal−alkyl species and corresponding metal−allyl complexes was furthermore confirmed in validation calculations on model reaction 2.

$$[H_2Ti(\eta^1\text{-}C_3H_7)]^+ = [H_2Ti(\eta^3\text{-}C_3H_5)]^+ + H_2 \quad (2)$$

The reaction energy calculated for (2) with the standard functional used in the present work (BPW91) is slightly lower than that obtained with a high-level ab initio method (CCSD(T)).[55]

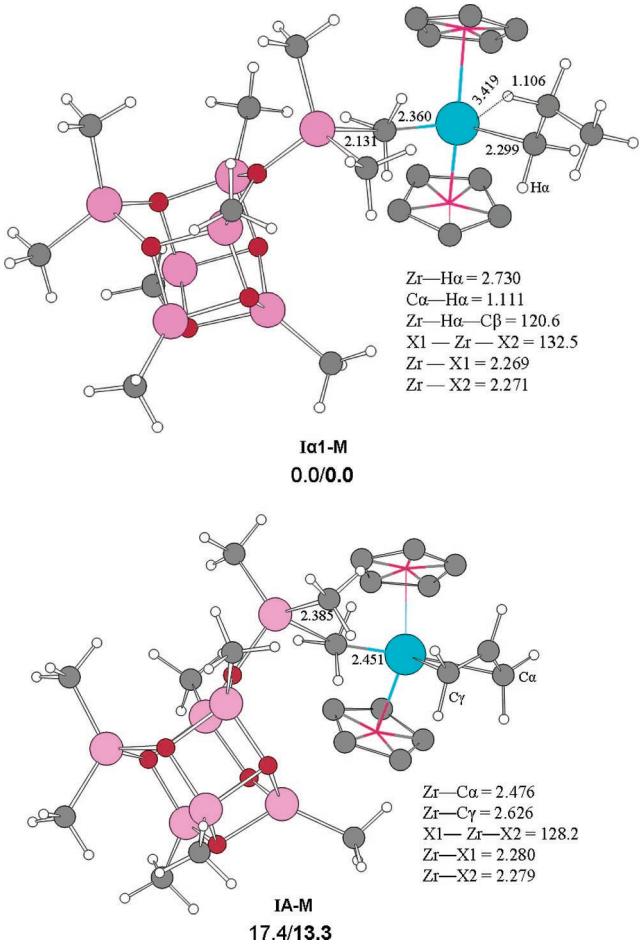

Figure 9. $[Cp_2Zr(\eta^1\text{-}C_3H_7)]^+TMA[MeMAO]^-$ (**Iα1-M**) and $[Cp_2Zr(\eta^3\text{-}C_3H_5)]^+TMA[MeMAO]^-$ (**IA-M**). Bond distances are given in angstroms, whereas energies are given in kcal/mol (ΔH_{298}/ΔG_{298}) relative to the primary alkyl (**Iα1-M**). The energy of **IA-M** also includes H_2. Hydrogen atoms of the Cp ligands have been omitted for clarity.

Finally, one may argue that the fine balance between the alkyl and allyl complexes could shift due to influence of the cocatalyst anion, and we have thus investigated also models of catalyst−cocatalyst adducts of **Iβ1** and **IA**. Zurek and Ziegler[30] have investigated a series of different adducts between $[Cp_2ZrMe]^+$, trimethylaluminum (TMA), and a model of methylated methylaluminoxane, $[MeMAO]^-$ (where MAO is modeled as the hexagonal cage structure $(MeAlO)_6$). We have adapted their most likely candidate for the active polymerizing species, $[Cp_2ZrMe]^+TMA[MeMAO]^-$ (structure C in ref 30), as starting points for optimization of the current alkyl- and allylzirconium complexes, $[Cp_2Zr(\eta^1\text{-}C_3H_7)]^+TMA[MeMAO]^-$ and $[Cp_2Zr(\eta^3\text{-}C_3H_5)]^+TMA[MeMAO]^-$. In the starting structure of $[Cp_2Zr(\eta^1\text{-}C_3H_7)]^+TMA[MeMAO]^-$ a β-agostic conformation was used for the alkyl chain, which, however, relaxed to give α-agostic conformation in the optimized structure (**Iα1-M** in Figure 9). The allyl structure, $[Cp_2Zr(\eta^3\text{-}C_3H_5)]^+TMA[MeMAO]^-$, retained the hapticity of the metal-bound allyl during optimization (**IA-M** in Figure 9). The catalyst−cocatalyst adducts investigated here show a clearer preference for the alkyl isomer, **Iα1-M**, than the naked cations do (vide supra). **IA-M** is more than 13 kcal/mol less stable than **Iα1-M** in terms of free energy. In summary, our calculations involving different conformers and isomers of the zirconium−alkyl species have not revealed structures that are predicted to be more stable than the β-agostic alkyl complexes, **Iβ1** and **IIβ1**. This further strengthens the hypothesis that dormant, or "slow", states originate from particularly stable configurations of catalyst−cocatalyst complexes.[29,30]

Conclusion

Density functional theory calculations on equilibria involving different conformations for zirconium alkyl cations $[L_2Zr-Pr]^+$ (L = Cp, Cp*; Pr = *n*-propyl) and subsequent insertion into the zirconium−propyl bond have not revealed a pattern matching that described for the single-center, two-state model.[28] For $[Cp_2Zr-Pr]^+$, the most stable of the ethylene-free complexes, the β-agostic conformer, is also the most reactive state with respect to ethylene coordination. For $[Cp^*_2Zr-Pr]^+$, the most facile route involves the γ- and α-agostic conformations of the alkyl complex, which thus at first glance appear to be candidate fast states, C_{fast}, but the barriers to rearrangement to the more stable β-agostic conformation are significantly lower than those of propagation.

Several isomerization reactions involving the propyl group of the $[L_2Zr-Pr]^+$ cation have been investigated in order to look for candidate slow states. For the most promising candidate slow state, these studies have also included a model of the MAO cocatalyst anion and high-level ab initio validation calculations. However, no structure was found to be of lower energy than the β-agostic conformation, and the latter thus takes the role of the resting state for both catalysts in the present study. Assuming that the single-center, two-state kinetic model applies to zirconocene-catalyzed ethylene polymerization, our failure to locate the corresponding fast and slow states suggests that these involve the cocatalyst anion. The slow, or dormant, states could be due to particularly stable configurations of catalyst−cocatalyst complexes, possibly originating from interactions with a catalyst featuring a growing polymer chain in favorable conformations. Accurate theoretical treatment of these complexes probably requires realistic models of (large) noncoordinating anions as well as inclusion of solvent effects.

The preferred pathways for the approach of ethylene are different in the two catalysts. For L = Cp, ethylene coordinates to the β-agostic resting state, whereas for L = Cp*, the favored propagation route involves ethylene approach to an α-agostic conformation. We anticipate that future studies will confirm the role of α-agostic or nonagostic conformations of the polymer chain in reducing the steric hindrance experienced by the incoming olefin, also in the case of other polymerization catalysts.

Acknowledgment. This work was supported by the European Commission through COST Action D17. We thank Prof. G. Fink, Dr. K. Angermund, Dr. H. Hermann, M. Graf, and H. U. Wüstefeld for valuable discussions.

Supporting Information Available: Energies and Cartesian coordinates of all optimized structures. This material is available free of charge via the Internet at http://pubs.acs.org.

References and Notes

(1) Jordan, R. F.; Dasher, W. E.; Echols, S. F. *J. Am. Chem. Soc.* **1986**, *108*, 1718. Jordan, R. F. *Adv. Organomet. Chem.* **1991**, *32*, 325.
(2) Silanes, I.; Ugalde, J. M. *Organometallics* **2005**, *24*, 3233.

(3) Aitola, E.; Surakka, M.; Repo, T.; Linnolahti, M.; Lappalainen, K.; Kervinen, K.; Klinga, M.; Pakkanen, T.; Leskela, M. *J. Organomet. Chem.* **2005**, *690*, 773. Yang, S. H.; Huh, J.; Yang, J. S.; Jo, W. H. *Macromolecules* **2004**, *37*, 5741. Kim, E. G.; Klein, M. L. *Organometallics* **2004**, *23*, 3319. Budzelaar, P. H. M. *Organometallics* **2004**, *23*, 855. Article: Borrelli, M.; Busico, V.; Cipullo, R.; Ronca, S.; Budzelaar, P. H. M. *Macromolecules* **2003**, *36*, 8171. Yang, S. H.; Jo, W. H.; Noh, S. K. *J. Chem. Phys.* **2003**, *119*, 1824. Wigum, H.; Solli, K. A.; Støvneng, J. A.; Rytter, E. *J. Polym. Sci., Part A: Polym. Chem.* **2003**, *41*, 1622. Martinez, S.; Cruz, V.; Munoz-Escalona, A.; Martinez-Salazar, J. *Polymer* **2003**, *44*, 295. Talarico, G.; Blok, A. N. J.; Wo, T. K.; Cavallo, L. *Organometallics* **2002**, *21*, 4939. Holscher, M.; Keul, H.; Hocker, H. *Macromolecules* **2002**, *35*, 8194. Borrelli, M.; Busico, V.; Cipullo, R.; Ronca, S.; Budzelaar, P. H. M. *Macromolecules* **2002**, *35*, 2835. Blom, R.; Swang, O.; Heyn, R. H. *Macromol. Chem. Phys.* **2002**, *203*, 381. Young, M. J.; Ma, C. C. M.; Ting, C. *Russ. J. Coord. Chem.* **2002**, *28*, 25. Lanza, G.; Fragala, I.; Marks, T. J. *Organometallics* **2001**, *20*, 4006. Linnolahti, M.; Pakkanen, T. A. *Macromolecules* **2000**, *33*, 9205. Rappé, A. T.; Skiff, W. M.; Casewit, C. J. *Chem. Rev.* **2000**, *100*, 1435. Thorshaug, K.; Støvneng, J. A.; Rytter, E. *Macromolecules* **2000**, *33*, 8136. Nifant'ev, I. E.; Ustynyuk, L. Y.; Laikov, D. N. *Russ. Chem. Bull.* **2000**, *49*, 1164. Petitjean, L.; Pattou, D.; Ruiz-Lopez, M. F. *J. Phys. Chem. B* **1999**, *103*, 27. Deng, L. Q.; Ziegler, T.; Woo, T. K.; Margl, P.; Fan, L. Y. *Organometallics* **1998**, *17*, 3240. Woo, T. K.; Margl, P. M.; Ziegler, T.; Blöchl, P. E. *Organometallics* **1997**, *16*, 3454. Musaev, D. G.; Froese, R. D. J.; Morokuma, K. *New J. Chem.* **1997**, *21*, 1269. Prosenc, M. H.; Brintzinger, H. H. *Organometallics* **1997**, *16*, 3889. Støvneng, J. A.; Rytter, E. *J. Organomet. Chem.* **1996**, *519*, 277. Margl, P.; Lohrenz, J. C. W.; Ziegler, T.; Blöchl, P. E. *J. Am. Chem. Soc.* **1996**, *118*, 8, 4434. Yoshida, T.; Koga, N.; Morokuma, K. *Organometallics* **1996**, *15*, 766. Yoshida, T.; Koga, N.; Morokuma, K. *Organometallics* **1995**, *14*, 746. Lohrenz, J. C. W.; Woo, T. K.; Fan, L. Y.; Ziegler, T. *J. Organomet. Chem.* **1995**, *497*, 91. Jensen, V. R.; Børve, K. J.; Westberg, N.; Ystenes, M. *Organometallics* **1995**, *14*, 4349. Bierwagen, E. P.; Bercaw, J. E.; Goddard III, W. A. *J. Am. Chem. Soc.* **1994**, *116*, 1481. Woo, T. K.; Fan, L.; Ziegler, T. *Organometallics* **1994**, *13*, 2252. Kawamura-Kuribayashi, H.; Koga, N.; Morokuma, K. *J. Am. Chem. Soc.* **1992**, *114*, 8687. Kawamura-Kuribayashi, H.; Koga, N.; Morokuma, K. *J. Am. Chem. Soc.* **1992**, *114*, 2359. Jolly, C. A.; Marynick, D. S. *J. Am. Chem. Soc.* **1989**, *111*, 7968.

(4) Vanka, K.; Xu, Z. T.; Ziegler, T. *Isr. J. Chem.* **2002**, *42*, 403.

(5) Moscardi, G.; Resconi, L.; Cavallo, L. *Organometallics* **2001**, *20*, 1918.

(6) Angermund, K.; Fink, G.; Jensen, V. R.; Kleinschmidt, R. *Chem. Rev.* **2000**, *100*, 1457. Angermund, K.; Fink, G.; Jensen, V. R.; Kleinschmidt, R. *Macromol. Rapid Commun.* **2000**, *21*, 91.

(7) Lohrenz, J. C. W.; Bühl, M.; Weber, M.; Thiel, W. *J. Organomet. Chem.* **1999**, *529*, 11.

(8) Margl, P. M.; Woo, T. K.; Blöchl, P. E.; Ziegler, T. *J. Am. Chem. Soc.* **1998**, *120*, 2174.

(9) Thorshaug, K.; Støvneng, J. A.; Rytter, E.; Ystenes, M. *Macromolecules* **1998**, *31*, 7149.

(10) Erratum: Thorshaug, K.; Støvneng, J. A.; Rytter, E.; Ystenes, M. *Macromolecules* **1998**, *31*, 9416.

(11) Woo, T. K.; Margl, P. M.; Lohrenz, J. C. W.; Blöchl, P. E.; Ziegler, T. *J. Am. Chem. Soc.* **1996**, *118*, 13021.

(12) Cossee, P. *J. Catal.* **1964**, *3*, 80. Arlman, E. J. *J. Catal.* **1964**, *3*, 89. Arlman, E. J.; Cossee, P. *J. Catal.* **1964**, *3*, 99.

(13) Ewen, J. A. *J. Mol. Catal. A: Chem.* **1998**, *128*, 103. Review: Brintzinger, H. H.; Fischer, D.; Mülhaupt, R.; Rieger, B.; Waymouth, R. M. *Angew. Chem., Int. Ed. Engl.* **1995**, *34*, 1143. Resconi, L.; Cavallo, L.; Fait, A.; Piemontesi, F. *Chem. Rev.* **2000**, *100*, 1253.

(14) Chen, E. Y. X.; Marks, T. J. *Chem. Rev.* **2000**, *100*, 1391. Jia, L.; Yang, X. M.; Stern, C. L.; Marks, T. J. *Organometallics* **1997**, *16*, 842.

(15) Vanka, K.; Xu, Z. T.; Ziegler, T. *Macromol. Symp.* **2004**, *213*, 275. Belelli, P. G.; Branda, M. M.; Castellani, N. J. *J. Mol. Catal. A: Chem.* **2003**, *192*, 9. Xu, Z. T.; Vanka, K.; Firman, T.; Michalak, A.; Zurek, E.; Zhu, C. B.; Ziegler, T. *Organometallics* **2002**, *21*, 2444. Zakharov, I. I.; Zakharov, V. A. *Macromol. Theor. Simul.* **2002**, *11*, 352. Lanza, G.; Fragala, I. L.; Marks, T. J. *Organometallics* **2002**, *21*, 5594. Schaper, F.; Geyer, A.; Brintzinger, H. H. *Organometallics* **2002**, *21*, 473. Lanza, G.; Fragala, I. L.; Marks, T. J. *J. Am. Chem. Soc.* **2000**, *122*, 12764. Vanka, K.; Chan, M. S. W.; Pye, C. C.; Ziegler, T. *Organometallics* **2000**, *19*, 1841. Braga, D.; Grepioni, F.; Tedesco, E.; Calhorda, M. J. *Z. Anorg. Allg. Chem.* **2000**, *626*, 462. Zakharov, V. A.; Talzi, E. P.; Zakharov, I. I.; Babushkin, D. E.; Semikolenova, N. V. *Kinet. Catal.* **1999**, *40*, 836. Beck, S.; Prosenc, M. H.; Brintzinger, H. H. *J. Mol. Catal. A: Chem.* **1998**, *128*, 41. Fusco, R.; Longo, L.; Proto, A.; Masi, F.; Garbassi, F. *Macromol. Rapid Commun.* **1998**, *19*, 257. Fusco, R.; Longo, L.; Masi, F.; Garbassi, F. *Macromolecules* **1997**, *30*, 7673. Fusco, R.; Longo, L.; Masi, F.; Garbassi, F. *Macromol. Rapid Commun.* **1997**, *18*, 433.

(16) Nifant'ev, I. E.; Ustynyuk, L. Y.; Laikov, D. N. *Organometallics* **2001**, *20*, 5375.

(17) Lieber, S.; Prosenc, M. H.; Brintzinger, H. H. *Organometallics* **2000**, *19*, 377.

(18) Jensen, V. R.; Børve, K. J.; Ystenes, M. *J. Am. Chem. Soc.* **1995**, *117*, 4109. Novaro, O.; Blaisten-Barojas, E.; Clementi, E.; Giunchi, G.; Ruiz-Vizcaya, M. E. *J. Chem. Phys.* **1978**, *68*, 2337. Armstrong, D. R.; Perkins, P. G.; Stewart, J. J. P. *J. Chem. Soc., Dalton Trans.* **1972**, 1972.

(19) Yang, X. M.; Stern, C. L.; Marks, T. J. *J. Am. Chem. Soc.* **1994**, *116*, 10015. Yang, X. M.; Stern, C. L.; Marks, T. J. *J. Am. Chem. Soc.* **1991**, *113*, 3623.

(20) Brandow, C. G.; Mendiratta, A.; Bercaw, J. E. *Organometallics* **2001**, *20*, 4253. Erker, G. *Acc. Chem. Res.* **2001**, *34*, 309. Dahlmann, M.; Erker, G.; Bergander, K. *J. Am. Chem. Soc.* **2000**, *122*, 7986.

(21) Casey, C. P.; Carpenetti, D. W. *Organometallics* **2000**, *19*, 3970. Wu, Z.; Jordan, R. F.; Petersen, J. L. *J. Am. Chem. Soc.* **1995**, *117*, 5867. Temme, B.; Erker, G.; Karl, J.; Luftmann, H.; Fröhlich, R.; Kotila, S. *Angew. Chem., Int. Ed. Engl.* **1995**, *34*, 1755.

(22) Ewen, J. A.; Elder, M. J.; Jones, R. L.; Curtis, S.; Cheng, H. N. In *Catalytic Olefin Polymerization*; Keii, T., Soga, K., Eds.; Kodansha: Tokyo, 1990; p 439. Herfert, N.; Fink, G. *Macromol. Symp.* **1993**, *66*, 157. Fink, G.; Herfert, N.; Montag, P. In *Ziegler Catalysts*; Fink, G., Mülhaupt, R., Brintzinger, H. H., Eds.; Springer-Verlag: Berlin, 1995; p 159. Chien, J. C. W.; Yu, Z. T.; Marques, M. M.; Flores, J. C.; Rausch, M. D. *J. Polym. Sci., Part A: Polym. Chem.* **1998**, *36*, 319. Oliva, L.; Pellecchia, C.; Cinquina, P.; Zambelli, A. *Macromolecules* **1989**, *22*, 1642. Suppl. 13: Pino, P.; Rotzinger, B.; Vonachenbach, E. *Makromol. Chem.* **1985**, 105.

(23) Jüngling, S.; Mülhaupt, R.; Stehling, U.; Brintzinger, H. B.; Fischer, D.; Langhauser, F. *Macromol. Symp.* **1995**, *97*, 205.

(24) Jüngling, S.; Mülhaupt, R.; Stehling, U.; Brintzinger, H. H.; Fischer, D.; Langhauser, F. *J. Polym. Sci., Part A: Polym. Chem.* **1995**, *33*, 1305.

(25) Schaper, F.; Brintzinger, H. H.; Kleinschmidt, R.; van der Leek, Y.; Reffke, M.; Fink, G. In *Organometallic Catalysts and Olefin Polymerization*; Blom, R., Follestad, A., Rytter, E., Tilset, M., Ystenes, M., Eds.; Springer-Verlag: Oslo, Norway, 2000; p 46.

(26) Ystenes, M. *J. Catal.* **1991**, *129*, 383. Ystenes, M. *Macromol. Symp.* **1993**, *66*, 71. Marques, M. M.; Costa, C.; Lemos, F.; Ribeiro, F. R.; Dias, A. R. *React. Kinet. Catal. Lett.* **1997**, *62*, 9. Munoz-Escalona, A.; Ramos, J.; Cruz, V.; Martinez-Salazar, J. *J. Polym. Sci., Part A: Polym. Chem.* **2000**, *38*, 571.

(27) Prosenc, M. H.; Schaper, F.; Brintzinger, H. H. In *Metalorganic Catalysts for Synthesis and Polymerization*; Kaminsky, W., Ed.; Springer-Verlag: Berlin, 1999; p 223.

(28) Fait, A.; Resconi, L.; Guerra, G.; Corradini, P. *Macromolecules* **1999**, *32*, 2104.

(29) Zurek, E.; Ziegler, T. *Prog. Polym. Sci.* **2004**, *29*, 107. Zurek, E.; Ziegler, T. *Faraday Discuss.* **2003**, *124*, 93.

(30) Zurek, E.; Ziegler, T. *Organometallics* **2002**, *21*, 83.

(31) Kaminski, E.; Fink, G., personal communication.

(32) Vosko, S. H.; Wilk, L.; Nusair, M. *Can. J. Phys.* **1980**, *58*, 1200.

(33) Becke, A. D. *Phys. Rev. A* **1988**, *38*, 3098.

(34) Perdew, J. P.; Wang, Y. *Phys. Rev. B* **1992**, *45*, 13244.

(35) Frisch, M. J.; Trucks, G. W.; Schlegel, H. B.; Scuseria, G. E.; Robb, M. A.; Cheeseman, J. R.; Zakrzewski, V. G.; Montgomery, J. A., Jr.; Stratmann, R. E.; Burant, J. C.; Dapprich, S.; Millam, J. M.; Daniels, A. D.; Kudin, K. N.; Strain, M. C.; Farkas, O.; Tomasi, J.; Barone, V.; Cossi, M.; Cammi, R.; Mennucci, B.; Pomelli, C.; Adamo, C.; Clifford, S.; Ochterski, J.; Petersson, G. A.; Ayala, P. Y.; Cui, Q.; Morokuma, K.; Malick, D. K.; Rabuck, A. D.; Raghavachari, K.; Foresman, J. B.; Cioslowski, J.; Ortiz, J. V.; Baboul, A. G.; Stefanov, B. B.; Liu, G.; Liashenko, A.; Piskorz, P.; Komaromi, I.; Gomperts, R.; Martin, R. L.; Fox, D. J.; Keith, T.; Al-Laham, M. A.; Peng, C. Y.; Nanayakkara, A.; Gonzalez, C.; Challacombe, M.; Gill, P. M. W.; Johnson, B.; Chen, W.; Wong, M. W.;

Andres, J. L.; Gonzalez, C.; Head-Gordon, M.; Replogle, E. S.; Pople, J. A. *Gaussian 98, Revision A.7*; Gaussian, Inc.: Pittsburgh, PA, 1998.

(36) Frisch, M. J.; Trucks, G. W.; Schlegel, H. B.; Scuseria, G. E.; Robb, M. A.; Cheeseman, J. R.; Montgomery, J. A., Jr.; Vreven, T.; Kudin, K. N.; Burant, J. C.; Millam, J. M.; Iyengar, S. S.; Tomasi, J.; Barone, V.; Mennucci, B.; Cossi, M.; Scalmani, G.; Rega, N.; Petersson, G. A.; Nakatsuji, H.; Hada, M.; Ehara, M.; Toyota, K.; Fukuda, R.; Hasegawa, J.; Ishida, M.; Nakajima, T.; Honda, Y.; Kitao, O.; Nakai, H.; Klene, M.; Li, X.; Knox, J. E.; Hratchian, H. P.; Cross, J. B.; Adamo, C.; Jaramillo, J.; Gomperts, R.; Stratmann, R. E.; Yazyev, O.; Austin, A. J.; Cammi, R.; Pomelli, C.; Ochterski, J. W.; Ayala, P. Y.; Morokuma, K.; Voth, G. A.; Salvador, P.; Dannenberg, J. J.; Zakrzewski, V. G.; Dapprich, S.; Daniels, A. D.; Strain, M. C.; Farkas, O.; Malick, D. K.; Rabuck, A. D.; Raghavachari, K.; Foresman, J. B.; Ortiz, J. V.; Cui, Q.; Baboul, A. G.; Clifford, S.; Cioslowski, J.; Stefanov, B. B.; Liu, G.; Liashenko, A.; Piskorz, P.; Komaromi, I.; Martin, R. L.; Fox, D. J.; Keith, T.; Al-Laham, M. A.; Peng, C. Y.; Nanayakkara, A.; Challacombe, M.; Gill, P. M. W.; Johnson, B.; Chen, W.; Wong, M. W.; Gonzalez, C.; Pople, J. A. *Gaussian 03*; Revision B.04 ed.; Gaussian, Inc.: Pittsburgh, PA, 2003.

(37) Jensen, V. R.; Børve, K. J. *J. Comput. Chem.* **1998**, *19*, 947.

(38) Becke, A. D. *J. Chem. Phys.* **1993**, *98*, 5648.

(39) Cizek, J. *Adv. Chem. Phys.* **1969**, *14*, 35. Purvis, G. D.; Bartlett, R. J. *J. Chem. Phys.* **1982**, *76*, 1910. Scuseria, G. E.; Janssen, C. L.; III, H. F. S. *J. Chem. Phys.* **1988**, *89*, 7382. Pople, J. A.; Head-Gordon, M.; Raghavachari, K. *J. Chem. Phys.* **1987**, *87*, 5968.

(40) Hay, P. J.; Wadt, W. R. *J. Chem. Phys.* **1985**, *82*, 299.

(41) Wadt, W. R.; Hay, P. J. *J. Chem. Phys.* **1985**, *82*, 284.

(42) Dunning, T. H.; Hay, P. J. In *Methods of Electronic Structure Theory*; Schaefer, H. F., Ed.; Plenum Press: New York, 1977; pp 1−27.

(43) Tobisch, S.; Ziegler, T. *J. Am. Chem. Soc.* **2004**, *126*, 9059.

(44) Wilhelm, E.; Battino, R. *Chem. Rev.* **1973**, *73*, 1.

(45) Pou-Amérigo, R.; Merchán, M.; Nebot-Gil, I.; Widmark, P.-O.; Roos, B. O. *Theor. Chim. Acta* **1995**, *92*, 149.

(46) The deviation from planarity for the three-coordinate metal complex, $[L_2Zr{-}Pr]^+$, is defined by the angle $\Xi = 360° - L^1ZrL^2 - L^1ZrPr - L^2ZrPr$.

(47) Frontside and backside attack refer to the approach of the ethylene molecule at the same side or opposite to the agostic hydrogen atom of the alkyl cation, respectively.

(48) No transition state on the potential energy surface of frontside coordination of ethylene to **Iα1** could be found. However, there exists a barrier (entropic in nature) on the free energy surface and an estimate of its magnitude was obtained by stepwise geometry optimization and vibrational analysis with a constrained Zr−C(ethylene) distance in order to locate the maximum on the free energy curve of ethylene coordination.

(49) Transition states of ethylene coordination may have slightly lower energies than those of separated reactants (propyl cation and free ethylene) due to the existence of weak charge-induced-dipole complexes at long Zr−ethylene distances. Even if the electronic energies of these complexes may be below the reactant asymptote, thermal and entropic corrections in practice render their enthalpies and free energies equal to or higher than the asymptote. These weak complexes are thus not important for the propagation kinetics of the title zirconocenes and their structures, and energies are therefore not reported.

(50) For L = Cp*, a propyl chain conformation similar to that in **Iα1** is not stable for the naked cations. However, there exist weak charge-induced-dipole complexes with this conformation. Rotation around the Cα−Cβ bond to interconvert between **Iα1** and **Iα2** was found to be associated with a low barrier. For L = Cp* such a rotation may take place, for example in the weak precoordination complex, prior to the TS of ethylene coordination ($[\mathbf{IIα2}{-}\mathbf{IIFα1}]^{‡}$).

(51) Döhring, A.; Jensen, V. R.; Jolly, P. W.; Thiel, W.; Weber, J. C. *Organometallics* **2001**, *20*, 2234.

(52) Lohrenz, J. C. W.; Woo, T. K.; Ziegler, T. *J. Am. Chem. Soc.* **1995**, *117*, 12793.

(53) Harvey, J. N. *Organometallics* **2001**, *20*, 4887.

(54) Hill, M.; Erker, G.; Kehr, G.; Fröhlich, R.; Kataeva, O. *J. Am. Chem. Soc.* **2004**, *126*, 11046.

(55) Using BPW91 (CCSD(T)) in connection with TZD2P basis sets, $\Delta E = 28.0$ (30.0) kcal/mol for reaction 2. The geometries were optimized using the BPW91 functional.

MA051224A